

Nonlinear trajectories in real-time fMRI using target volumes

Bruno Riemenschneider¹, Pierre Levan¹, Marco Reisert¹, and Jürgen Hennig¹

¹University Medical Center Freiburg, Freiburg, Germany

Target audience: The presented method is designed for real-time fMRI applications with a low number of predefined volumes of interest.

Purpose: Real-time fMRI has the requirement of fast image reconstruction for subsequent data analysis, and so forbids the expensive iterative reconstructions of undersampled nonlinear trajectories inhering high temporal resolution during the fMRI measurement. However, it is shown that when restricting the reconstruction to a number of volumes, the average time series of the signal from within the volumes can be computed efficiently. Using precalculations, the signal from one volume can then be obtained by a single scalar product in the signal domain. This enables to estimate the activation in the target volumes, while the whole dataset of undersampled data remains available for extensive retrospective analysis. The advantages of nonlinear trajectories are consequently accessible to real-time fMRI studies.

Methods: The target volumes V_i need to be determined before the real-time scan, e.g., from a functional prescan with paradigm, using ICA, using standard atlases or anatomical constraints. For the reconstruction of the average time series two methods were investigated:

1) The complex sum over all voxels contained in V_i can be expressed via the scalar product $\langle V_i, \mathbf{m} \rangle = \langle V_i, \mathbf{E}_{rec} \mathbf{s} \rangle$, where the signal equation $\mathbf{s} = \mathbf{Em}$ relates the signal \mathbf{s} and the image \mathbf{m} via the forward operator \mathbf{E} , and \mathbf{E}_{rec} represents the reconstruction operator. When \mathbf{E}_{rec} is linear, the scalar product can be rewritten as $\langle \mathbf{E}_{rec}^* V_i, \mathbf{s} \rangle$, where $*$ denotes the conjugate transpose. This means that after calculation of all $\mathbf{E}_{rec}^* V_i$ the summed signal from all V_i can be retrieved from signal space via one matrix product (Method 1a). This formulation also permits to include an image phase for each voxel in V_i in order to minimize intra-volume dephasing effects. The phases can be obtained by one reconstruction $\mathbf{E}_{rec} \mathbf{s}$ from a prescan prior to the reconstructions $\mathbf{E}_{rec} V_i$ (Method 1b).

2) Another option is to use a strongly simplified signal equation $\mathbf{s} = \mathbf{Av}$, similar to the method suggested by Wong¹, that maps the MR signal straight to the predefined volumes. In this approximation the elements of the encoding matrix are $A_{ni} = \int w_i(r) e^{jk_n r} dV \approx \sum_m E_{nm} w_i(x_m)$, where the weighting factors w_m define the volumes. Here, the number of volumes was chosen to be 90, i.e., all volumes of the functional ROI atlas². After its calculation, the matrix \mathbf{A} is small enough to be inverted via direct pseudo-inverse.

A simulation (fig. 2) of a complex time series was used to investigate generic effects of both methods, and method 1 was applied exemplary to a real time series of a functional scan with visual stimulus. The first frame of the real time series served as underlying image for the simulation data. The latter was created by random amplitude BOLD modulation at maximal 5% of the subjected voxels' intensity. These voxels were contained in volumes of the functional ROI atlas, coregistered with a prescan, and gaussian pink noise with spatial correlation was adjusted such that the average contrast-to-noise ratio (CNR) over all BOLD-modulated voxels was 1. Both real and simulated data were a 32-channel signal from a single shot sub-100ms stack-of-spirals trajectory³ (fig. 1). The nuFFT-based forward operator was used for the creation of the simulation data, as well as the reconstructions. The latter, if not by direct pseudo-inverse, was performed minimizing a cost-function using a conjugate gradient method with 20 iterations.

As reference time series for each volume in the simulation, the absolute values from the voxels inside each volume were averaged prior to simulating the measurement.

Results: In fig. 3 the CNR from each method relative to the reference CNR is plotted over volumes. To account for the random distribution of BOLD amplitudes inside the volumes, only those with more than 50 voxels have been considered. The light red line represents a measure of spatial phase coherence inside each volume, ranging from 0 to 1, calculated from the first frame via $1/N_i \sum_{n \in V_i} m_n / \text{abs}(m_n)$, N_i being the number of voxels inside V_i . The average CNR over all plotted volumes using the different methods are: 1.2 (reference), 0.94 (1b), 0.72 (1a) and 0.51 (2). Fig. 4 shows a reconstruction of the real time series averaged over a part of the visual cortex. The pink line represents the time series reconstructed via method 1a, the black line represents the sum of absolute values obtained via conventional frame-by-frame reconstruction. The ratio of CNR in both time series is 1.0.

Discussion: The CNR values of Method 1b) are highest in all volumes, where those of Method 2 are lowest. Only with

decreasing phase coherence the CNR values of Method 1a and 1b show significant differences. The average CNR of Method 1b is the near the overall average of 1.

Conclusion: The investigated methods show potential to extract information from nonlinear trajectories in rtMRI, which could be used for neurofeedback studies. Assuming the volume of activation is known before the feedback measurement, method 1 shows reasonable average CNR values with options for improvement in case the ROI is prone to intra-volume dephasing.

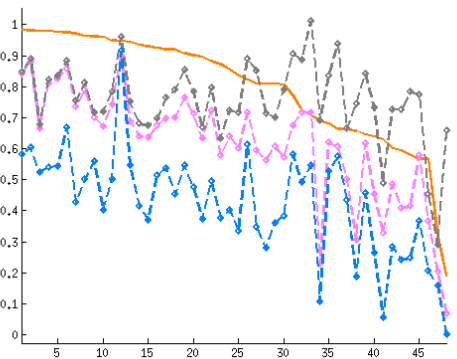


Figure 3: CNR values in a selection of volumes, relative to the CNR of the reference timeseries. Method 1a in pink, 1b in black, 2 in blue. The light red line indicates a measure of spatial phase coherence, ranging from 0 to 1, in the volumes.

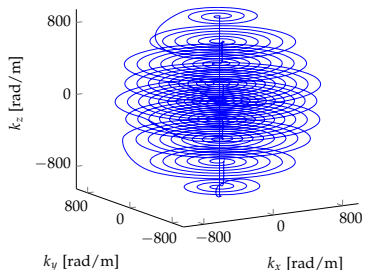


Figure 1: Single shot stack-of-spirals trajectory

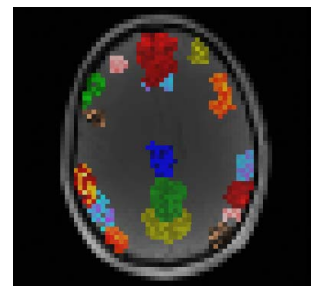


Figure 2: t-values of the simulation. Each volume of the atlas with own colormap

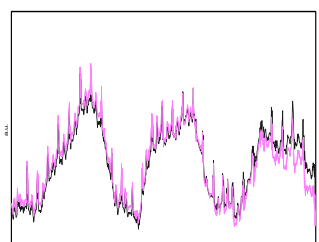


Figure 4: Real time series averaged over a part of the visual cortex. Reconstructed via method 1a (pink) and frame-by-frame (black)

References: 1. Wong, Brain Connectivity 2014, 4(7): 481-86, 2. Shirer et al., Cereb Cortex. 2012, 22(1):158-65, 3. Assländer et al., Neuroimage 2013, 3:59-70

Acknowledgement: This work was supported by the ERC Advanced Grant 'OVOC' grant agreement 232908.